Safety and Health at Work 8 (2017) 237–245

Contents lists available at ScienceDirect

Safety and Health at Work

journal homepage: www.e-shaw.org

Review Article

Hazards Caused by UV Rays of Xenon Light Based High Performance Solar Simulators

Gerd Dibowski*, Kai Esser

German Aerospace Center (DLR e.V.), Institute of Solar Research, Cologne, Germany

ARTICLE INFO

Article history:
Received 23 December 2015
Received in revised form
22 February 2016
Accepted 13 December 2016
Available online 25 January 2017

Keywords:
solar furnace
solar simulator
ultraviolet light
xenon short arc lamp

ABSTRACT

Background: Solar furnaces are used worldwide to conduct experiments to demonstrate the feasibility of solar–chemical processes with the aid of concentrated sunlight, or to qualify high temperature-resistant components. In recent years, high-flux solar simulators (HFSSs) based on short-arc xenon lamps are more frequently used. The emitted spectrum is very similar to natural sunlight but with dangerous portions of ultraviolet light as well. Due to special benefits of solar simulators the increase of construction activity for HFSS can be observed worldwide. Hence, it is quite important to protect employees against serious injuries caused by ultraviolet radiation (UVR) in a range of 100 nm to 400 nm.
Methods: The UV measurements were made at the German Aerospace Center (DLR), Cologne and Paul-Scherrer-Institute (PSI), Switzerland, during normal operations of the HFSS, with a high-precision UV-A/B radiometer using different experiment setups at different power levels. Thus, the measurement results represent UV emissions which are typical when operating a HFSS. Therefore, the biological effects on people exposed to UVR was investigated systematically to identify the existing hazard potential.
Results: It should be noted that the permissible workplace exposure limits for UV emissions significantly exceeded after a few seconds. One critical value was strongly exceeded by a factor of 770.
Conclusion: The prevention of emissions must first and foremost be carried out by structural measures. Furthermore, unambiguous protocols have to be defined and compliance must be monitored. For short-term activities in the hazard area, measures for the protection of eyes and skin must be taken.

1. Introduction

Solar furnaces are used to carry out chemical, thermal, and material experiments, where highly concentrated sunlight is used for industrial applications instead of fossil or nuclear fuels. Solar furnaces of different power and sizes are in operation worldwide, varying from small to large scale as per examples below. Fig. 1 shows the small scale facility of the National Renewable Energy Laboratory, USA and Fig. 2 the large scale facility in Odeillo, France.

The medium sized plant of the German Aerospace Center (DLR) in Cologne (Fig. 3) concentrates sunlight by a factor of 5,000 to a total power of 25 kW. A radiation of E up to 5 MW/m^2 onto an experimental setup and temperatures up to 2,770 K can be achieved. The core applications of this process are testing and evaluating experiments in the field of basic research as per industry demands. High-temperature solar thermochemical cycles and assessment of materials under conditions of extreme temperature and radiation intensity will be carried out. The DLR high-flux solar simulator (HFSS) was put into operation in 2007 to support the solar furnace. The HFSS is an assembly of 10 elliptical aluminum reflectors which consists of xenon short arc lamps with an artificial light spectrum close to natural sunlight (Fig. 4), which enables the user to perform the same experiments in principle as in a solar furnace.

The emitted short wave (optical) radiation of about 20 kW is concentrated on a target at a distance of 3 m. The radiation sums up to a heat flux E = 4 MW/m^2. The lamps used (Osram 6,000 W/HSLA Ozone Free (OFR)) are ozone free, which means that wavelengths below 280 nm will be suppressed [1]. With a HFSS it is possible to carry out long-term experiments and to reproduce a spectral radiant composition of a former experiment. Because xenon lamps offer a very stable emission spectrum regardless of operating time and age of the lamp, tests for qualification purposes can be carried

* Corresponding author. German Aerospace Center (DLR e.V.), Institute of Solar Research, Linder Hoehe, D-51147 Cologne, Germany.
E-mail address: gerd.dibowski@dlr.de (G. Dibowski).

2093-7911/$ – see front matter
http://dx.doi.org/10.1016/j.shaw.2016.12.002

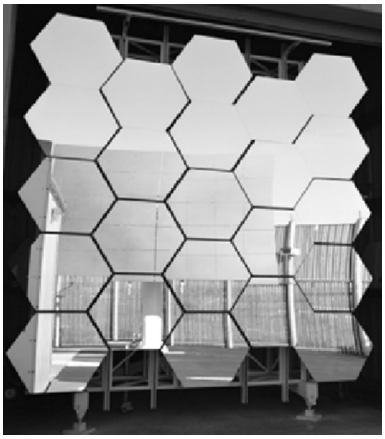

Fig. 1. The 10 kW high-flux solar furnace of the National Renewable Energy Laboratory, Golden, USA.

Fig. 2. The 1 MW (world's largest) solar furnace of the CNRS Font Romeu Odeillo, France. CNRS, Centre National de la Recherche Scientifique.

out e.g., for ceramic absorbers at different time periods. The flux is controlled by a so-called 'shutter'. It consists of a number of water-cooled metal plates which rotate around the vertical axis.

1.1. Worldwide increase in the use of solar simulators

Due to the identified specific benefits of solar simulators compared to solar furnaces, an increasing number of these systems are coming into operation worldwide. In addition, by the end of 2016, the world's largest solar simulator *SynLight* consisting of 159 xenon-lamps will be completed at the DLR solar test-site in Juelich 70 km west of Cologne. As far as we are aware, its total power will

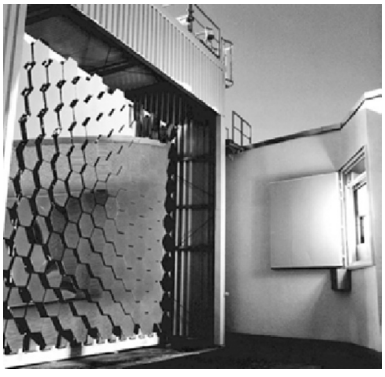

Fig. 3. The 25 kW solar furnace of the German aerospace center, DLR, Cologne, Germany.

Fig. 4. The Cologne high-flux solar simulator of the German aerospace center under operation.

be greater than the sum of all individual outputs of systems worldwide [2].

A collection of known HFSS with solar radiant powers above 10 kW in comparison with *SynLight* is shown in Table 1.

2. Materials and methods

Ultraviolet radiation (UVR) plays a significant biological role because individual photon energies are the greatest within the optical spectrum. The energy of a photon increases with decreasing wavelength. These short wave, higher energy photons have sufficient energy to produce photochemical alterations that may initiate potentially injurious biological effects.

Both beneficial and unwanted photo-biological effects result from UVR exposure. The critical organs in terms of UVR exposure are the eye and the skin, as they may be readily exposed [9]. UV-B is biologically much more effective in comparison to UV-A. A total of 1,000 to 10,000 times more photons of UV-A are necessary in order to cause the same effect as UV-B [10].

Xenon lamps, which are almost always used in solar simulators, emit a dangerous amount of UVR. Without appropriate safeguards the radiation on uncovered skin soon leads to burns, eye damage, and permanently enhances the risk for cancer. Nevertheless, xenon lamps are used for special purposes such as in cinema projectors, drying of glues, sterilization, or as light sources for scientific applications.

The EU-Directive 2006/25/EC [11] describes that in many processes with optical radiation the permissible workplace exposure limits (ELs) of UV emissions have been reached after seconds!

Aengenvoort [12] and Wang [13] state that, depending on the welding method, the limit of the irradiance within the UV-A/B/C can even be reached at an exposure period of less than 1 s. Despite the high-risk potential of UVR emitted from the HFSS and hence its enormous hazard potential for unprotected employees, no hazard assessments exist.

For this reason a systematic metrological examination and analysis of the possible UV exposure onto employees near the HFSS during current experiments were performed at the DLR in Cologne and at the Paul-Scherrer-Institute, Switzerland [14]. The comprehensive measurements of UVR exposure were taken under realistic conditions during the running experiments and are presented and discussed below.

2.1. Hazard potential to the human eye

UVR exposure onto the eye is absorbed by the cornea and the lens. In the case of excessive exposure to UVR the human eye reacts with photokeratitis and photoconjunctivitis (light-induced inflammation of the cornea or conjunctiva). Symptoms range from

Table 1
SynLight and the known HFSS equipped with xenon lamps and solar radiant powers > 10kW

Location	YoC	Focal length (m)	Electric power (kW)	Radiative power (kW)	Heat flux (MW/m^2)	Source
DLR, Jülich, D	2016	8.0	149 × 7	300	≤11.0	[2]
ANU, AUS	2015	1.9	18 × 2.5	8.4	3.0	[3]
EPFL, CH	2015	1.9	18 × 2.5	8.4	3.0	[3]
GaTech, USA	2015	2.5	7 × 6	6.1	4.9	[4]
ETHZ, CH	2014	2.5	7 × 6	10	3.2	[5]
KTH, S	2014	1.5	12 × 7	10.6	3.75	[6]
Niigata Univ., JP	2013	3.0	19 × 7	~ 30	~ 0.95	[6]
AUTh, Gr	2013	3.0	11 × 6	20	4.8	[2]
IMDEA, Madrid, E	2013	2.5	7 × 6	14	3.6	[7]
UF, USA	2011	2.0	7 × 6	14	5.0	[8]
UMN, USA	2010	2.3	7 × 6.5	9.2	<3.24	[6]
DLR, Cologne, D	2007	3.0	10 × 6	18	4.0	[1]
PSI, CH	2005	3.0	10 × 15	50	11	[2]
N China Electric U	n/a	n/a	7 × n/a	n/a	n/a	[6]

YoC, year of commissioning.

mild irritation, light sensitizing and tearing, to severe pain, which subside after a few days. Chronic UV-A and UV-B exposure may result in protein changes in the lens, leading to cataract. The entire risk potential is shown in Table 2 [15].

2.2. Hazard potential to the human skin

Due to the working conditions the problem can be focused on the facial skin, because the body skin is usually well protected.

However, a clear description of precise limits is difficult because there are very different sensitive skin types, such as “melano-compromised” or “melano-competent”. The details are described by the International Congress of Non-Ionizing Radiation Protection [16].

When evaluating UV-related skin damage, the wavelength range between 250 nm and 400 nm is particularly weighted, since it emits erythema-effective radiation. This is the area which is particularly capable of harming the human skin, like erythema caused by sunburn is a possible trigger of skin cancer, as this is preceded by DNA damage [17]. In summary, the risks can be divided as illustrated in Table 2 according to Swerdlow [9] and DIN German Institute for Standardization [18].

2.3. Mathematical description of the biological effect

In order to determine the effects of UVR on the eye and skin, the wavelength-dependent depletion potential has to be biologically weighted. This is done with the relative spectral effectiveness S(λ) for modifying the biological effective irradiance, which is shown in Fig. 5 [13,16].

It shows that UV-A radiation has almost no biologically active effect. UV-C radiation was not fully included in the measurement, since the resulting UV-C radiation from the xenon lamp is to be completely shielded by the quartz bulb, yet still a significant biological activity prevails in this area. The measuring range by means of the UV-B sensor, which can measure up to 240 nm in the UV-C, was also detected.

Table 2
Risks for the eyes and skin from UV-rays

Wavelength (nm)		Eye	Skin
100–280	UV-C	Photokeratitis Photoconjunktivitis	Erythema Skin cancer
280–315	UV-B	Photokeratitis Photoconjunktivitis Cataractogenesis	Erythema Elastosis Skin cancer
315–400	UV-A	Cataractogenesis	Skin cancer

It can be shown that the greatest potential of hazards for the eye and skin are in the UV-B-range. The most critical amount, its peak, is in UV-C at 270 nm [13,19]. Irradiation with UV-light of this wavelength quickly reaches and exceeds the recommended limits issued by the International Commission on Non-Ionizing Radiation Protection (ICNIRP) [16].

Thus, the range of 240 nm to 300 nm of UVR exposure is important for the measurement campaign. To evaluate the biological effectiveness [16] a table of the weighting factors S(λ) for wavelengths between 180 nm and 400 nm was issued. If these factors are multiplied by the energy of the wavelengths, the result is the biologically effective portion of the UV rays (Table 3).

2.4. Formulae of the limit value calculation

The biological weighted yield-size radiant exposure H_S in J/m^2, which results from the sum of the single irradiation power E_S in mW/m^2 over a time period of 8 hours, is the main reference for assessment of the exposure dose of UVR.

To determine the permissible biologically weighted irradiation limit the weighting factors S(λ) will be used. Based on the ICNIRP data [16] the following equations are valid:

$$H_s = \int_{\Delta t_{exp}} E_s(t)\,dt \tag{1}$$

with

$$E_s = \int_{\lambda_1}^{\lambda_2} E_\lambda(\lambda) \cdot S(\lambda)\; d\lambda \tag{2}$$

simplified:

$$H_{eff} = E_{eff} \cdot \Delta t \tag{3}$$

with:
H_S: biological weighted exposure; H_{eff}: effective exposure (J/m^2); E_S: biological weighted power; E_{eff}: effective power (mW/m^2); dt/Δt: time of exposure (s).

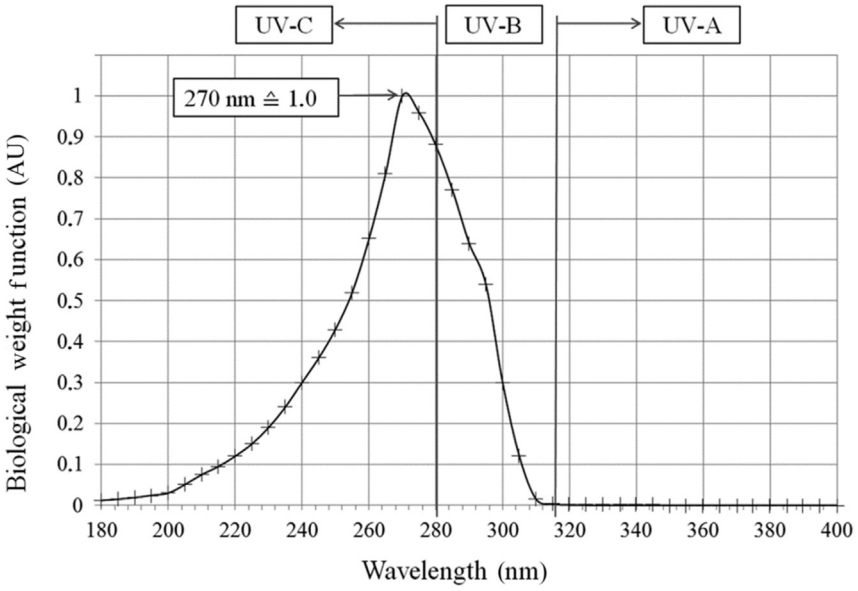

Fig. 5. Relative spectral effectiveness S(λ) for biologically effective UV light and normalized to 1 at 270 nm.

2.5. Exposure limits

According to the recommendations for protection by Wang et al [13] and the ICNIRP [16] for both general and occupational exposure to UVR upon the skin or eye within an 8 hour period, the ELs are listed in Table 4.

UVR incidents in the spectral biologically weighted area from 180 nm to 400 nm on unprotected eye(s) should not exceed 30 J/m^2 using the spectral weighting factors contained in Table 3. The total (unweighted) UV radiant exposure in the spectral region 315 nm to 400 nm (UV-A) should not exceed 10^4 J/m^2 [16].

Permissible exposure time to a UVR incident upon unprotected skin or eye can be calculated by dividing 30 J/m^2 by the value of E_{eff} in W/m^2, e.g., (30 Ws/m^2)/(5 W/m^2) = 6 s [Eq. (3)].

Table 5 illustrates the allowed exposition times as a function of the effective irradiance E_{eff} [15].

Table 3
Spectral UV exposure limits (J/m^2) and weighting function S(λ) (dimensionless) of UV in the range of 240 nm to 315 nm

λ* (nm)	EL (J/m^2)	S(λ)†	λ* (nm)	EL (J/m^2)	S(λ)†
240	100	0.300	280‡	34	0.880
245	83	0.360	285	39	0.770
250	70	0.430	290	47	0.640
255	58	0.520	295	56	0.540
260	46	0.650	300	100	0.300
265	37	0.810	305	500	0.060
270	30	1.000	310	2,000	0.015
275	31	0.960	315	10,000	0.003

For the entire range of UV-B a weighting average value S(280; 315) can be calculated: 0.31833.
Excerpt from ICNIRP (IRPA). International Commission on Non-Ionizing Radiation Protection of the International Radiation Protection Association. 2004. Guidelines on Limits of Exposure to Ultraviolet Radiation of wavelengths between 180 nm and 400 nm (incoherent optical radiation). Health Phys 2004;87:171–86.
EL, exposure limits.
* Wavelengths chosen are representative; other values should be interpolated [see Eqs. (1–3)].
† Relative spectral effectiveness.
‡ Wavelength < 280 nm blocked by the lamp design.

Table 4
Emission limit values for noncoherent optical radiation (UV) on a daily exposure time of 8 h

	UV-A, UV-B, UV-C	UV-A*
Range of wavelengths λ (nm)	180–400	315–400
With S(λ) biologically weighted allowable exposure limit of the spectral irradiation (J/m^2)	H_{eff} = 30	H_{eff} = 10,000
Effective irradiance (mW/m^2)	E_{eff} = 1	E_{eff} = 347
All working days per year (J/m^2)	H_{eff} = 4,000	

* Biological weighting not necessary (see Fig. 5).

2.6. Measurement boundary conditions

The UV measurements at DLR and the Paul-Scherrer-Institute (PSI), Switzerland, have been made during the regular operation of the HFSS, in different reflective experiment setups with variable power levels. Therefore, the measurement results reflect UV emissions typical for application. Fig. 6 demonstrates a typical setup with light source, experimental setup, and the operator under influence of UV radiation.

Experimental setups mostly reflect a large part of the impinging radiation back to the surroundings due to metallic or white (aluminium-oxide ceramic insulation material) surfaces. Experience shows that these are typical setup configurations, which are transferable to other solar simulators (and furnaces) in general. Considering this, four measuring positions were selected (Fig. 7).

Table 5
Limiting UV exposure durations based on exposure limits

Duration of exposure per day	Effective irradiance E_{eff} (W/m^2)
8 h	0.001
4 h	0.002
1 h	0.008
30 min	0.017
5 min	0.1
30 s	1.0
1 s	30
0.1 s	300

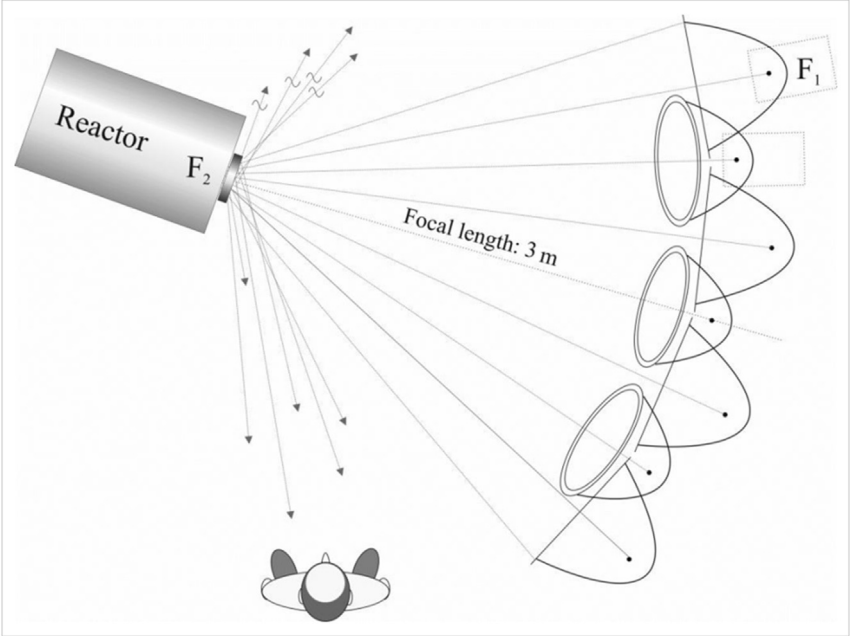

Fig. 6. Hazardous position for employees under realistic operating conditions.

For the first series of measurements the positions were located as described in Fig. 7. Being irradiated during a running experiment could be the case, for example, when a cooling pipe is leaking, opening or closing of a valve is needed, a device has to be switched, or a sudden error occurs.

2.7. Applied measurement device

The high precision radiometer RM 21 (OpSyTec, Germany) was used. This instrument measures the irradiance and dose rate with a resolution of 0.1 mW/cm^2 (UV-A) and 0.01 mW/cm^2 (UV-B). Ambient light can be effectively corrected by an automatic offset. The integrated diffusers provide the required cosine correction. The sensors are calibrated with traceability to the National Metrology Institute of Germany (PTB), postcalibratable and are delivered with a work-calibrating certificate. The measurement accuracy is specified by the manufacturer for both measuring heads with ±7 %. For the measurement campaign the measuring heads have been bought new and have therefore been calibrated.

2.8. Rotation sensitivity of the measuring head

The sensitivity as a function of the viewing angle was checked before starting the measurement campaign. The measuring heads were rotated towards the lamps in steps of 4°. The zero point was defined in each case as the point where the largest expected radiation appeared. Within a measuring cone of 5°, the measured value can be accepted as almost constant. For larger angles the measurement errors increased strongly.

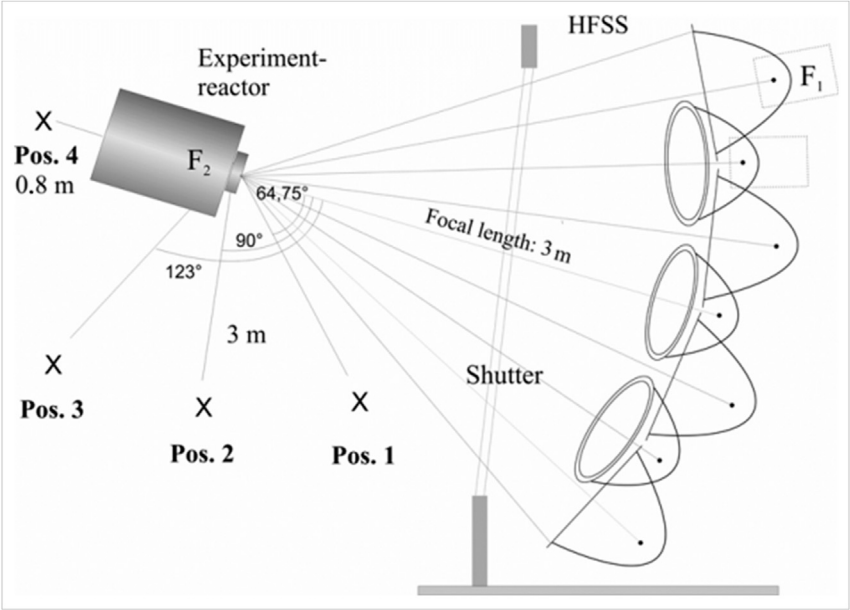

Fig. 7. Measuring positions at the German Aerospace Center high-flux solar simulator. HFSS, high-flux solar simulator.

3. Results

The specified measurement series examines the radiation exposure under realistic experimental conditions. Based on more than 20 years of operational experience of the main author, experimental reactors are often similar; the currently used reactor represents the average appropriate. Therefore a certain transferability of the results to similar constellations at other HFSSs is given.

3.1. Measurement at Position 1

The 10 lamps with the designations from A1 to C3 were switched on stepwise to show the time behavior (Table 6). The spectrum of the lamps changed in the first 10 to 15 minutes after ignition, causing a rise in UV emission. After reachuing the steady-state, individual measuring points were repeatedly measured up to one hundredfold. In this series of measurements the middle and top lamp series (B- and C-series) were used, while the shutter was opened to 100%. Due to reconstruction work on the lamps of the A-series, they could not be used.

It is evident that the lamps which are more oriented towards the viewer have a stronger effect (B1 to B4) than the more averted lamps (C1 to C3). Even at the radiation levels that occur during the operation of a single lamp (2.5 $KW_{opt.}$), the recommended limits determined by the ICNIRP [16] are exceeded.

Lamp C1 exceeded the limit value for the irradiance at Position 1 175 times. The lowest measured value (C3) exceeded the limit 44.37 times. For all seven lamps in operation an excess of the limits of 770 times (over an 8 h working period) could been proven.

3.2. Measurements at Position 2

For Position 2 similar results as for Position 1 were expected. The maximum permissible exposure time was measured after 1,351 s. This corresponds to the 22.2 times of the permissible limit, based on a constant irradiation over eight working hours. The significantly longer exposure time is plausible as the reflectance is significantly lower at 90° towards the measuring head than at Position 1.

3.3. Position 3: all lamps depending on the opening degree of the shutter (7 lamps)

At Position 3 (123° deflection to the optical main-axis) the total load as a function of the opening degree of the shutter is described in Table 7. The UV exposure increases significantly with gradual opening of the shutter.

Table 6
Determination of the permissible UV-power load E (mW/m^2) at Position 1

Position of lamp*	UV-B (W/m^2) measured	UV-B† (W/m^2) biologically weighted	Maximum of allowable† exposure duration (s)
B1	0.50309	0.16015	187
B2	0.32199	0.10250	293
B3	0.27745	0.08832	340
B4	0.25782	0.0820	366
C1	0.54980	0.17501	171
C2	0.16418	0.05226	574
C3	0.1394	0.04437	676

* Due to reconstruction work on the A-line, only the B- and C-lines were measured.
† Correlated to the weighting function $S(\lambda)_{UV-B} = 0.318\overline{3}$ (Table 3).
Example: $t_{max} = H_{eff}/E_{eff}$ [Eq. (3)], $(30\ J/m^2)/(0.16015\ Js^{-1}/m^2) = 187$ s. This would give lamp B1 an allowed maximum exposition time of 187 s.

Table 7
Determination of the permissible UV-power load E (mW/m^2) at Position 3

Shutter position (%)	UV-B (W/m^2) measured	UV-B (W/m^2) biologically weighted	Maximum of allowable exposure duration (s)
50	0.52909	0.16842	178
60	1.63393	0.52013	58
70	2.11317	0.67269	45
100	2.62200	0.83466	36

3.4. Position 4: behind the experimental setup

Concluding the series of measurements at the DLR-HFSS with specified measurement positions, the radiometers were positioned at the optical axis 0.8 m behind the reactor. Therefore, the instrument received only scattered radiation. Depending on the real experimental boundary conditions it was possible to measure at shutter positions of 70% and 80% opening degree (Table 8).

Directly behind the experimental setup, the UV exposure is similar to that at measurement Position 3. In spite of multiple reflection, the UV-B output reaches comparatively high values of 1.9 W/m^2 and 2.1 W/m^2.

At this position the duration of stay is not allowed for longer than 14 s and 49 s, depending on the shutter opening degree. The results at this point are higher than assumed for only measuring scattered light. The experimenter must thus assume that even scattered radiation is far from harmless due to white room walls or metallic reflecting surfaces.

3.5. UV measurements at PSI

PSI is the largest research institute for natural and engineering sciences within Switzerland. The main research topics are material, energy, environment, and human health. Like the DLR, the PSI operates a solar furnace and a solar simulator. As a longstanding partner of DLR, PSI made it possible for the authors to take UV measurements at their solar simulator (Fig. 8) [14]. The construction of the PSI's HFSS is similar to the DLR-HFSS. Both are made of an array of 10 Lamps in similar arrangement, however, the PSI uses lamps and reflectors in bigger dimensions.

The most significant difference between the HFSS at the DLR and the one at the PSI is a glass pane between the shutter and the experiment. This pane is made of low iron solar glass.

The measuring positions of the first test series were located at a distance of 2 m to the focal point. On this radius are five measuring points in total. A second test series was performed to measure the radiation behind the experiment. The measuring points are lined perpendicular to the optical axis 3.5 m behind the focus. The experiment setup consists of a down beam-receiver. This means the

Table 8
Determination of the permissible UV-power load E (mW/m^2) behind the experiment at Position 4 (scattered radiation)

Shutter position (%)	UV-B (W/m^2) measured	UV-B (W/m^2) biologically weighted	Maximum of allowable exposure duration (s)
70	1.92673	0.61334	49
80	2.09307	0.66633	14

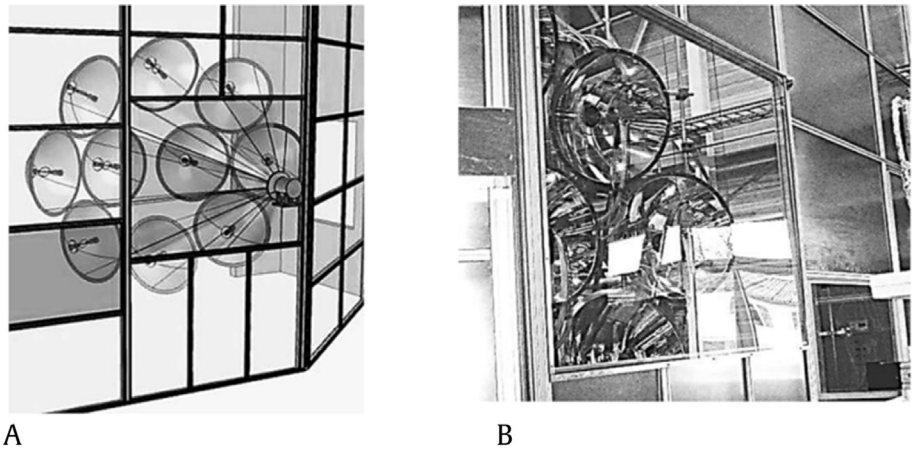

Fig. 8. Schematic of Paul-Scherrer-Institute's solar simulator. (A) Protective housing of the lamp array and a window pane to the control room. (B) View of lamp/reflector array with one lamp in operation behind a protective window pane.

beam is deflected by a tilted mirror into the receiver. Since the experimental reactor resembles a funnel, the scattered radiation around the reactor is estimated to be minor.

3.6. Measuring Series 1 at PSI

Four measuring points were defined at PSI on one side of the experiment (Fig. 9). These resembled the measurements at DLR in Cologne in a distance of 2 m from the focus and in angles ranging from 75° to 139° to the optical axis. Test Position 1 was exactly defined in the center of the window in the splinter protection wall.

As seen in Table 9, the UV load rises with a decreasing angle between measuring device and optical axis. The testing Positions 5 and 6 are the same as Position 2, but the sensor is pointed parallel to the optical axis for Position 5 and directly to one lamp through the solar glass window pane in the splinter protection wall. The values are between 27 and 180 times higher than the limit. Furthermore, it is shown that the glass pane has only little to no effect on UV reduction.

3.7. Measuring Series 2 at PSI

During the second test series at PSI eight measuring points were defined in a straight line perpendicular to the optical axis, 3.5 m behind the focus. The points were defined at a distance of 50 cm to each other, five points to the right and three points left of the optical axis. The radiation emission exceeded the limit by the factor of 10 to 21. After all, the measured radiation values are comparatively low. The EL of the daily dose recommendation by the ICNIRP [16] is exceeded after 23 minutes at the point of highest load. The lower radiation is explained by the bigger distance in the experiment, since the radiation decreases in proportion to the square of the distance to the radiation source (reciprocal distance rule) and by the mirror blocking the biggest part of the radiation. Since the solar simulator at PSI is placed in a much larger hall compared to the DLR, wall reflections and scatter radiation are lower. This does not lead to the conclusion that lower amounts of radiation do not need the same degree of protection than in bigger facilites. In every case one should avoid any windowed surfaces, use cameras as the only means to monitor the experimental space, use metal lining on simulator enclosures, control ducting and ventilation of the simulator enclosure, and other recommendations like [3], [5] or [20].

3.8. Error calculation

The inaccuracies to consider are: the measurement errors of the instrument, the wrong deflection of the measuring heads, and spacing errors. The sensors have a calibrated inaccuracy of 7%. In addition, the positional inaccuracy is assumed to be 1 cm; according to the distance law this results in a mistake of 1.9 %. The

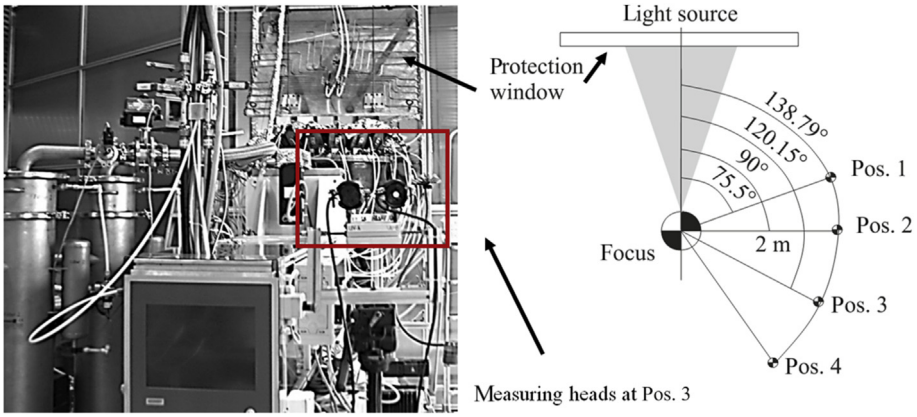

Fig. 9. Experimental setup Paul-Scherrer-Institute, Switzerland; measurement positions test Series 1 PSI.

Table 9
Determination of the UV exposure limits E (mW/m^2) at PSI

Measuring position	Angle (°)	UV-B (W/m^2) measured	UV-B (W/m^2) biologically weighted	Maximum of allowable exposure duration (s)
1	75.52	0.63171	0.20109	149
2	90.00	0.32387	0.10310	291
3	120.19	0.14085	0.04484	670
4	138.59	0.09736	0.03100	968
5 (2)	90.00	0.41392	0.13176	228
6 (2)	90.00	0.49645	0.15804	190

angle inaccuracy can be accepted by the authors experience as 0.25 %. which leads to a total error of 9.46 % for the measuring value.

4. Discussion

The technical use of high concentrated sunlight for a future global CO_2-free energy supply is of outstanding importance. Besides generating electricity, industrial processes can also be carried out, for example, the production of chemical products or tests of high temperature-resistant materials.

Scientific research studies will take place worldwide at solar furnaces, or increasingly at solar simulators. The light of these simulators is based almost always on xenon short arc lamps because its spectrum is very similar to the sun. It has become clear that the UV light component in an open environment exposes people to questionably high or seriously damaging effects.

Consequently, experiments were carried out in an extensive measurement campaign to access the biological hazard potential caused by reflections from metallic or mirrored surfaces in regards to immediate surroundings. In summary, it should be noted that the permissible workplace ELs for UV emissions is significantly exceeded in a matter of seconds. Dangerous or unacceptable levels of radiation were obtained at most thresholds, including extreme critical values exceeded by a factor of 770. In areas of reflected radiation ELs are also exceeded.

However, by employing the biological weighting algorithm S(λ) it should be noted that UV-B emission within the range of 280 nm to 315 nm and with a small part of UV-C, a pathogenic effect arises.

Here the ELs are almost always obtained in less than a minute. However, no biologically effective radiation is caused by UV-A.

Furthermore, it can be shown that with the partition glass pane between the lamps and the experiment (at PSI HFSS), closing the mandatory existing protective housing has only little to no effect on the reduction of UV emissions. For reasons of various scientific objectives this pane is not necessary.

Preventing the emissions of most commonly used xenon lamps at solar simulators must be resolved by structural measures. Furthermore, unambiguous protocols must be defined by the acting authority, with compliance regulary monitored. Commission guidelines for protective measures must be consistently followed.

Based on the two case studies presented and an analysis of published geometrical and power characteristics of other HFSSs, it is recommended that such devices are always hosted inside dedicated UV-proof enclosures, while humans are not exposed to direct, reflected, and/or scattered simulated radiation during the facility operation.

This leads to the conclusion that, in general, based on the international experience of solar simulator employment, any human presence should be strictly forbidden in the vicinity of a HFSS, irrespective of the power output or geometry of a facility. UV screens and enclosures without windows are recommended to host these facilities.

Conflicts of interest

All authors declare that there are no conflicts of interest.

Acknowledgments

The authors thank the DLR solar furnace team C. Willsch, M. Thelen and Dr. C. Raeder for technical support, S. Breuer, the experimenter on HFSS during the UV- measurements who supported us despite the existing disturbances, as well as Dr. Ivo Alxneit and Dr. Christian Wieckert of Paul-Scherrer-Institute PSI, Villigen, Switzerland, who enabled us to take measurements there to give the final statement content of this publication even more weight.

References

[1] Dibowski G, Neumann A, Rietbrock P, Willsch C, Säck JP, Funken KH. DLRs new high-flux solar simulator-fundamentals, technology, application. Institute of Solar Energy. Proceedings of the 10th Solar Colloquium, vol. 11. Cologne, Germany; 2007. p. 67–8.
[2] Wieghardt K, Funken KH, Dibowski G, Hoffschmidt B, Laaber D, Hilger P, Eßer K. Synlight -The world's largest artificial sun. Proceedings of the 21st Solar Paces Conference, vol 21. Cape Town, South Africa; 2015. p. 153–7.
[3] Bader R, Haussener S, Lipinski W. A 45 kWe multi-source high-flux solar simulator. Sol Energy Eng 2014;137:12–21.
[4] Gill R, Bush E, Haueter P, Loutzenhiser P. Characterization of a 6 kW high-flux solar simulator with an array of xenon arc lamps capable of concentrations of nearly 5000 suns. Rev Sci Instrum 2015;86:125107.
[5] Li J, Gonzalez-Aguilar J, Romero MH. Line-concentrating flux analysis of 42 kW high-flux solar simulator. International Conference on Concentrating Solar Power and Chemical Energy Systems [Internet]. SolarPACES; 2014. Available from: http://www.solarpaces.org/press-room.
[6] Bader R, Levêque G, Haussener S, Lipiński W. High-flux solar simulator technology. OSA Light, Energy and the Environment Congress, Leipzig, 14–17 November 2016. OCIS codes: (350.6050) Solar energy; (230.6080) Sources.
[7] Li J, Gonzalez-Aguilar J, Pérez-Rábago C, Zeaiter H, Romero HM. Optical analysis of hexagonal 42kWe high-flux solar simulator. Energ Proc 2014;57:590–6.
[8] Erickson B, Petrasch J. High Flux Solar Simulator for the Investigation of Solar Thermo-chemical Cycles at Low Pressures [Internet]. Poster presentation at FESC Summit, Orlando, USA; 2010. Available from: http://floridaenergy.ufl.edu/wp-content/uploads/Solar-Fuels-for-Thermochemical-PETRASCH.pdf.
[9] Swerdlow AJ. Health Effects from Ultraviolet Radiation. Chilton, Oxfordshire, Great Britain: Report of the Advisory Group on non-ionizing Radiation of the National Radiological Protection Board NRPB [Internet]. 2002. 282 p. [cited 2014 Jan 23]. Available from: https://www.gov.uk/government/uploads/system/uploads/attachment_data/file/414185/NRPB_Doc_series_vol13_no1.pdf
[10] CIE Commission International de ÍEclairage. Erythemale Referenzwirkungsfunktion und standardisierte Erythemdosis. Standardization of the terms UV-A1, UV-A2 and UV-B. Vienna; 1999. Report CIE-134/1. 55 p.
[11] EU-Richtlinie 2006/25/EG über Mindestvorschriften zum Schutz von Sicherheit und Gesundheit der Arbeitnehmer vor der Gefährdung durch physikalische Einwirkungen (künstliche optische Strahlung) [EU Directive 2006/25/EC on minimum requirements for the protection of safety and health of employees from the risks arising from physical impacts (artificial optical radiation)]. Bruxelles: European Parliament and Council. 2006. Guideline 89/391/EWG: 38-44. 20 p. [in German].
[12] Aengenvoort B, Schwaß D. BGIA-Report 3/2007, UV-Strahlenexpositionen an Arbeitsplätzen. Institut für Arbeitsschutz der Deutschen Gesetzlichen Unfallversicherung [UV radiation exposure to working places. Institute for Occupational Safety and Health of the German Social Accident Insurance]. Sankt Augustin, Germany; 2007. 44 p. [in German].
[13] Wang F, Gao Q, Hu L, Gao N, Ge T, Yu J, Liu Y. Risk of Eye Damage from the Wavelength-Dependent Biologically Effective UVB Spectrum Irradiances [Internet]. Plos One, USA; 2012. [cited 2015 Apr 11]. Available from: http://journals.plos.org/plosone/article?id=10.1371%2Fjournal.pone.0052259.
[14] Alxneit I, Dibowski G. Solar Simulator Evaluation Report. EU-Project SFERA Solar Facilities for the European Research Area. Font Romeu Odeillo. France; 2011. Deliverable 12.5. 35 p, SFERA, funded by the European Commission under Contract No. 385228296.
[15] Siekmann H. Carcinogenic potential of solar radiation and artificial sources of UV radiation. Institut für Arbeitsschutz der Deutschen Gesetzlichen Unfallversicherung (IFA) [Institute for Occupational Safety and Health of the German Social Accident Insurance] [Internet]. Sankt Augustin; Germany; 2011. 8 p. [cited 2016 Feb 13]. Available from: http://www.dguv.de/medien/ifa/en/fac/strahl/pdf/carcinogenic_potential_uv.pdf
[16] ICNIRP (IRPA) International Commission on Non-Ionizing Radiation Protection of the International. Radiation Protection Association. 2004. Guidelines on

Limits of Exposure to Ultraviolet Radiation of wavelengths between 180 nm and 400 nm (incoherent optical radiation). Health Phys 2004;87:171–86.
[17] Armstrong BK, Kricker A. The epidemiology of UV induced skin cancer. University of Sydney. J Photochem Photobiol B 2001;63:8–18.
[18] DIN EN 14255-1. Messung und Beurteilung von personenbezogenen Expositionen gegenüber inkohärenter optischer Strahlung. Teil 1: von künstlichen Quellen am Arbeitsplatz emittierte ultraviolette Strahlung. DIN Deutsches Institut für Normung e.V. [Measurement and assessment of personal exposures to incoherent optical radiation. Part 1: ultraviolet radiation emitted by artificial sources at the workplace. DIN German Institute for Standardization]. Beuth Verlag Berlin; 2005. 33 p. [in German].
[19] BGl 5006: Expositionsgrenzwerte für künstliche optische Strahlung. 2004. Berufsgenossenschaft der Feinmechanik und Elektrotechnik. Fachausschuss "Elektrotechnik" der DGUV [Exposure limits for artificial optical radiation. Employer's Liability Insurance Association for Precision Mechanics and Electrical Engineering. Technical Committee "Electrical engineering" of DGUV]. Cologne; 2004. 63 p. [in German].
[20] Leveque G, Bader R, Lipinski W, Haussener S. Experimental and numerical characterization of a new 45 kWel multisource high-flux solar simulator. Opt Express Oct. 2016;24(22):1360–73.